[Frontiers in Bioscience 12, 1946-1955, January 1, 2007]

Electrochemical studies oxidation of ciprofloxacin at nano-SnO_2/PVS modified electrode and its interaction with calf thymus DNA

Yuejuan Cai , Yuzhong Zhang, Shao Su, Shuping Li, Yonghong Ni

College of Chemistry and Materials Science, Anhui Key Laboratory of Functional Molecular Solids, Anhui Normal University, Wuhu 241000, P.R. China

TABLE OF CONTENTS

1. ABSTRACT

In pH 6.0 phosphate buffer solutions (PBS), a glassy carbon electrode (GCE) modifying by nano-tin oxide/ poly vinyl sulfonic potassium (nano-SnO_2/PVS) exhibited an enhanced effectiveness for the oxidation of ciprofloxacin (CFX), which compared with a bare GCE or a nano-SnO_2 modified electrode. In addition we also investigated the electrooxidation mechanism of the fluoroquinolone antibiotics (utilizing ciprofloxacin, ofloxacin, sparfloxacin and lomefloxacin) at the modified electrode. Further more, Gel electrophoresis coupled with electrochemistry and spectra techniques were used to study the interaction of CFX and calf thymus DNA (ctDNA). These acquired data showed that the binding mode of CFX and DNA was mainly an intercalation mechanism.

2. INTRODUCTION

Recently nano-materials have attracted much attention and have been widely used in material, electronic, physical fields for various purposes due to their unique properties. Nano-SnO_2 possesses excellent photoelectronic properties, high gas sensitivities and a short response time as well as relatively higher conductivity than TiO_2 and SiO_2 (1-3). These new kinds of inorganic nanomaterials exhibit tunable porosity, high thermal and chemical stability. Up to now, some inorganic oxide nanomaterials have been investigated in fundamental studies of protein-electrode interactions and the development of biosensing devices (4-14). The nanoporous structures of these inorganic oxide films greatly enhance the active surface area available for protein binding. These films facilitate direct electron

transfer process between biomolecules and electrodes. In the work, SnO_2 nanocrystals were synthesized by the hydrothermal method. We used the nano-SnO_2 to modify a GCE and investigated the electrochemical behavior of CFX at the nano-SnO_2 modified GCE.

CFX belongs to the family of fluoroquinolone antibacterial agents that also includes norfloxacin, ofloxacin and some other molecules. These fluoroquinolone antibacterial agents are synthetic derivatives of 6-fluoro-4-oxo-quinoline-3-carboxylic acid. They are fluorinated at position 6 and mostly bear a piperazinyl moiety at position 7. Ciprofloxacin is one of the most potent quinolone derivatives in clinical use with a very broad spectrum of antibacterial activity and is often used as an antibacterial agent of last resort (15). Although the exact mechanism of fluoroquinolone pharmacological action is still unclear, numerous studies had shown that the drug binding to DNA (16–18) and gyrase (19) was enhanced in the presence of Mg^{2+} and that Mg^{2+} was essential for antibacterial efficiency of drug–DNA interaction. Fluoroquinolone binding to the gyrase–DNA complex might prevent the religation step (16, 20–23). The mechanism of fluoroquinolone's inhibition of religation and the role of DNA in drug binding remains to be resolved. Understanding the interactions between fluoroquinolone and DNA might help to elucidate the action mechanism of this class of antibacterial agents. In this paper, we studied the electrochemical behavior of CFX at nano-SnO_2 modified GCE and investigated the interaction of CFX and DNA by electrochemistry, UV/Vis absorbance spectra, fluorescence spectra and gel electrophoresis. These obtained data indicated the binding mode of CFX and DNA was mainly an intercalation mechanism.

3. EXPERIMENTAL PROCEDURES

3.1. Reagents

Calf thymus DNA (sodium salt, type I) was obtained from Sigma (USA) and was used without further purification. Its purity was confirmed by UV/Vis absorption, which produced A_{260}/A_{280} value of approximate 1.8-1.9, suggesting the DNA sample was free proteins. The stock solution of DNA was directly dissolved in water and stored at 4 °C. The DNA concentration per nucleotide (DNA-P) was determined spectrophotometrically (24) at 260 nm by using the extinction coefficient 6600 cm^{-1} M^{-1}. CFX was purchased from Chinese National Institute for the Control of Pharmaceutical and Biological Products (purity >90.0%) and was used without further purification. Poly (vinyl) sulfonic potassium was purchased from Fluka. Other chemicals were analytical reagent. All solutions were prepared with double-distilled water.

3.2. Apparatus

Transmission electron microscopy (TEM) images of nanoparticles were acquired on a Hitachi H-600 0(Tokyo) transmission electron microscopy. Ethanol solutions of the nanoparticles were dropped on 50 Å thick carbon-coated copper grids with the excess solution being immediately whisked away.

The X-ray diffraction (XRD) patterns of the nano-SnO_2 were operated on a D/MAX-6000 powder diffractometer. (Rigaku CO. Germany).

Cyclic voltammograms (CVs) were obtained on a CHI 660 electrochemical workstation (Shanghai ChenHua Instruments, China) with a three-electrode system. A platinum wire was used as auxiliary electrode, a saturated calomel electrode (SCE) as a reference electrode, a bare or nano-SnO_2/PVS film modified glassy carbon electrode (GCE) (Ø=3.2 mm) as a working electrode, respectively. All potentials were reported to the SCE.

The UV/Vis absorbance spectra were acquired on U-3010 spectrofluorometer (Hitachi, Japan) equipped with a quartz micro-colorimetric vessel of 1cm path length.

Fluorescence spectra and relative fluorescence intensities were measured on a model F-4500 fluorescence spectrophotometer (Hitachi, Japan) equipped with a xenon lamp, dual monochromators, and a 1 cm × 1 cm quartz cell. The slit-width for both excitation and emission was set at 5 nm.

Agarose gel electrophoresis was attained on a general WC horizontal and UV-2000 analysis instrument (Shanghai Tianneng company, China).

3.3. Electrode preparation

A bare GCE was successively polished in the Al_2O_3 slurry from 0.3 to 0.5 μm before modification. Then it was rinsed with double distilled water and sonicated in 1:1 nitric acid, acetone and double distilled water for 10 min, respectively. Then the electrode was activated by continuous cyclic scanning 15 circles in 1.0 M sulfuric acid solution between -0.1 and +1.6 V with a rate of 100 mV/s and allowed to dry at room temperature.

For preparing a nano-SnO_2 and PVS film modified GCE, a nano-SnO_2 suspension was obtained by dispersing 10.0 mg nano-SnO_2 into 10 ml PVS solution. The 6 μL suspension was dropped onto the surface of clean GCE. Then solvent was evaporated in the air, the final electrode was taken as nano-SnO_2/PVS/GCE. A PVS/GCE (dropping 6μL PVS solution), a nano-SnO_2 /GCE (dropping 6 μL nano-SnO_2 suspension) and a bare GCE were taken to compare. All measurements were performed in a 10 ml electrolytic cell with 5 ml solutions, where oxygen was removed with high-purity nitrogen for 20 min. All sample solutions were deoxygenated by bubbling N_2 gas before each experiment.

4. RESULTS AND DISCUSSION

4.1. Preparation and characteristics of nano-SnO_2

4.1.1 The preparation of nano- SnO_2

In this paper, nano-SnO_2 was synthesized by the hydrothermal synthesis, using $SnCl_4 \cdot 5H_2O$ as the precursor. 0.8790 g $SnCl_4 \cdot 5H_2O$ was dissolved in the mixing solution of 10 ml glycol and 50 ml water, adjusted the solution pH

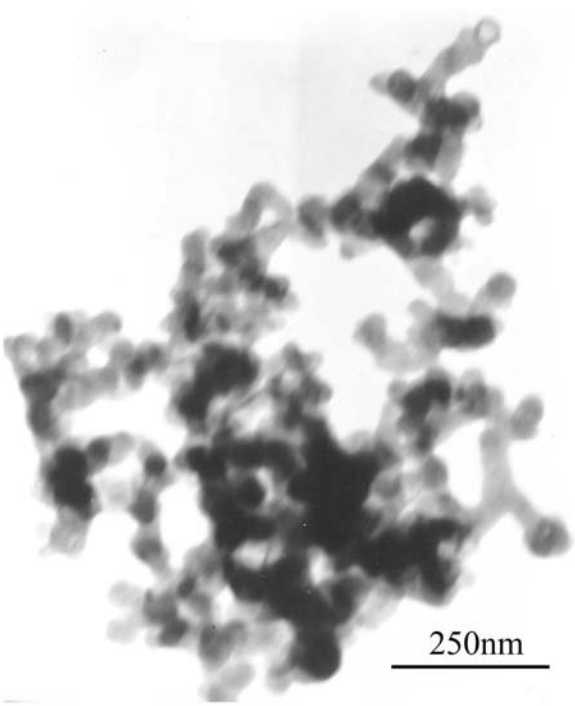

Figure 1. The TEM image of the nano-SnO_2.

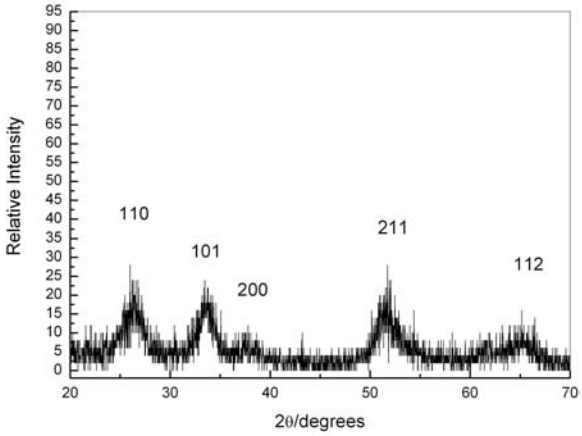

Figure 2. X-ray diffraction patterns of the nano-SnO_2.

to 1, and then reacted 24 h at 150 °C. The products were washed by ethanol and dried at 80°C.

4.1.2. The characteristics of nano-SnO_2

Figure 1 shows the typical TEM image of the nano-SnO_2. The particles are homogeneous with the average diameter of 15–20 nm. Figure 2 shows the X-ray diffraction patterns of the nanoparticles prepared. We could see that the 2θ peaks are agreement with the diffraction patterns from (110), (101), (200), (211) and (112) planes.

4.2. Electrochemical behaviors of CFX at the nano-SnO_2 modified electrode

4.2.1. Cyclic voltammograms of CFX at various modified electrode

Figure 3A shows the CVs at the nano-SnO_2/PVS/GCE in pH 6.0 PBS without CFX. No redox peak was observed in blank solution. Figure 3B depicts the CVs of CFX at the nano-SnO_2/PVS/GCE (curve d), nano-SnO_2/GCE (curve c), PVS/GCE (curve a) and bare GCE (curve b) in pH 6.0 PBS, respectively. At a bare GCE (curve b) and PVS/GCE (curve a), the electrochemical responses of CFX were very poor. However at nano-SnO_2 modified electrode (curve c), it shows a good electrochemical response, the peak current was enhanced; meanwhile the oxidation peak negatively shifted, The reason ascribe to the great surface area of nano-SnO_2 (25). At the nano-SnO_2/PVS electrode (curve d), the anodic peak current was higher than that at the nano-SnO_2 modified electrode. The one reason could be that nano-SnO_2/PVS film had negative charge, so it could attractive positive charge CFX, because ciprofloxacin exists as a cation below pH 5, when the pH is between 5 and 10, it is as a mixture of anions, cations and zwitterions, and it is as an anion over than pH 10 (26–29). So it could attract more CFX to electrode surface than it at bare electrode, so peak current is increased. Another reason was that PVS film could provide a favorable microenvironment for CFX and facilitates the electron exchange (25). From the CVs we could conclude that the electrode reaction of CFX is irreversible at nano-SnO_2/PVS film modified electrode.

In addition, the effect of the scan rate on the peak current of CFX was investigated. The anodic peak currents were proportional to scan rates over the range of 80~260 mV/s. The Linear regression equation was $i_{pa}(\mu A)= 0.5012 + 0.0062\ v$ (mV/S) with a correlation coefficient of r=0.9980; meanwhile we also investigated the effect of accumulation time on the peak currents, the experiment result shows that the peak current increases with the accumulation time till five minutes, which suggested that the electrode reaction of CFX at nano-SnO_2/PVS film modified electrode was an adsorption-controlled process.

4.2.2. Effect of pH

The effect of the solution pH on electrochemical response of CFX was investigated over the range of 2.0~8.0. Figure 4A shows that the anodic peak potential negatively shifted with increasing solution pH. The fact indicates protons take part in the electrode process. From Figure 4B, we could also observe the peak current increases with pH value of solution from 2.0 to 6.0. When pH>6.0, the anodic peak current decreases and peak shape becames worse. When pH>7.0, the electrooxidation of CFX almost could not happen. From the changes of peak shape and peak current of CFX, we selected pH 6.0 PBS as the supporting electrolyte. These data showed the electrooxidation of CFX easily occurred in the acid solution.

4.2.3. Determination of CFX

The determination of CFX concentration was performed with differential pulse voltammetry (DPV). The oxidation peak current of CFX was selected as the analytical signal. The result shows that the anodic peak current is proportional to the concentration of CFX over the range of 1.2×10^{-8} ~5.0×10^{-5} M, and the linear regression equation is ip_a (10 μA)=0.3243 + 0.0065C (μM), with a correlation coefficient of r=0.9988. The detection limit

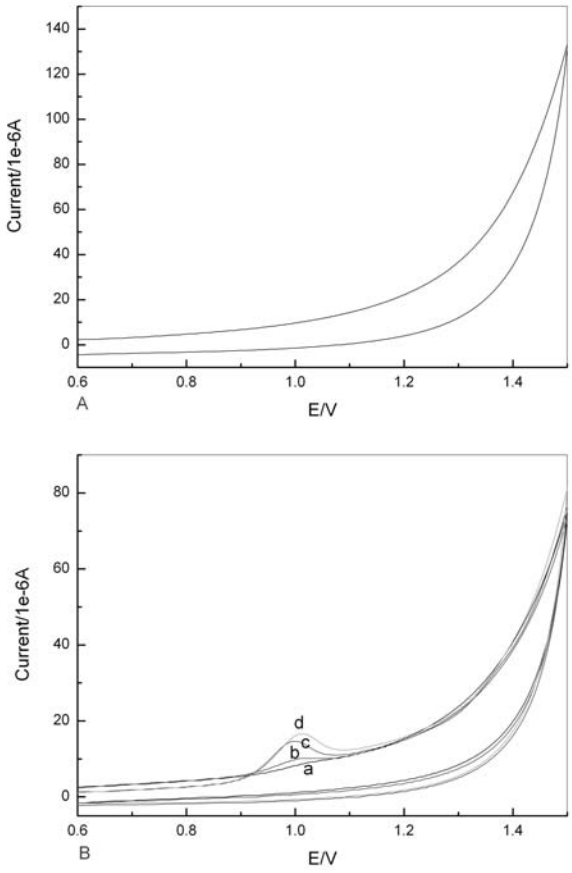

Figure 3. A: Cyclic voltammograms of nano-SnO_2/PVS modified GCE in 0.1M PBS (pH 6.0) without CFX.
B: Cyclic voltammograms of 1×10^{-5} M CFX in 0.1M PBS (pH 6.0) at different electrodes: (a) PVS film modified GCE; (b) the bare GCE; (c) nano-SnO_2 modified GCE; (d) nano-SnO_2/PVS modified GCE. The scan rate is 100 mV/S.

(S/N=3) is 6.0×10^{-9} M. To the same surface of a nano-SnO_2/PVS film modified electrode, the relative standard deviation of 10 scans is 2.4% for 1×10^{-5} M CFX, indicating excellent reproducibility of the modified electrode.

Furthermore, we also investigated the stability of the modified electrode. The peak current of same concentration CFX could hardly change after storage in air in at least 3 weeks or cyclic scanning 400 circles in PBS to the same surface of a nano-SnO_2/PVS film modified electrode.

4.2.4. Eletrooxidation mechanism of CFX

To an adsorption-controlled irreversible process, basing on the equation of E_p versus lnν: $E_p = E^0 + (RT/\alpha nF)\ \ln(RTK_s/\alpha nF) - (RT/\alpha nF)\ \ln\nu$. We could obtain the slope of the equation: $0.0257/\alpha n=0.0269$, where α, n were electron transfer coefficient and electron number taking part in reaction, respectively, with a correlation coefficient of r=0.9987. Given α to be 0.5, then n=1.93≈2. Then according to the equation: $dE_p/dpH=-0.059x/\alpha n$, where x was the number of hydrogen ions taking part in the reaction process, we calculated x to be 0.89≈1. We could conclude that one hydrogen ion and two electrons probably took part in the electrode reaction. This result was agreement with the values Smyth and Ivaska (30) determined other piperazine moiety, such as flurazepam and chlordiazepoxide. Another study on trazodone and nefazodone with piperazine ring was realized by CVs, DPV and SWV at the GCE, the oxidation process was also similar (31, 32). Taking into account that the CVs of the above molecules closely matched the CVs of CFX, we might postulate that the oxidation steps of CFX were located on the piperazine moiety which represented a typical oxidation system with two electrons oxidation process in acidic media. We might assume that the electrooxidation of the nitrogen occurred when the nitrogen of the piperazine ring, distal to the molecule, was protonated.

For further supporting the electrooxidation mechanism, we investigated other fluoroquinolone antibacterial agents, such as ofloxacin (OFX), sparfloxacin (SPX) and lomefloxacin (LMF). The CVs and schemes of these drugs are showed in Figure 5. We might see the peak potential is similar; furthermore the relationship of pH-dependent is similar under the acidic media condition. When pH >7.0, the electrochemical oxidation of these drugs almost could not happen. The CVs of SPX was especially and had two anodic peaks, the first peak and the second peak should be responding to the 5-position amidogen and the nitrogen of the piperazine ring oxidation, respectively. In addition piperazine hydrochloric acid also was operated at a bare GCE and had an approximative peak potential. The data more indicate the electrooxidation of fluoroquinolone drugs occur on the piperazine moiety. The electrode reaction (representation by CFX) as follows:

4.3. Studying the interaction between CFX and ctDNA

4.3.1. Electrochemical investigating the interaction between CFX and ctDNA

Fig.7 shows the CVs of CFX at a nano-SnO_2/PVS /GCE in pH 6.0 PBS in the absence of ctDNA or in the presence of ctDNA. The oxidation peak current of CFX obviously decreased in the presence of ctDNA. The phenomenon indicates that the interaction of ctDNA and CFX exists. However the peak potential is very stable. The result shows the interaction of ctDNA and CFX is different from metal ion and organic small molecule produce metal complex (The peak potential of the metal complex usually is different from that of the metal ion).

4.3.2. Investigating UV/Vis absorption spectra

Spectroscopic techniques are very useful tools to gain important information in biological science (33). Spectroscopic investigation of the interaction of CFX and ctDNA may be beneficial to clarifying the interaction mechanism. The interaction of CFX and ctDNA in PBS (pH 6.0) could be further confirmed by UV/Vis spectra. The variation of adsorption spectroscopy is presented in Figure 8. For the spectrum of free CFX, an absorption band was observed at 272 nm and 323 nm (curve a). However, in the presence of ctDNA, the 323 nm absorption peak of CFX red shifted and the absorption intensity

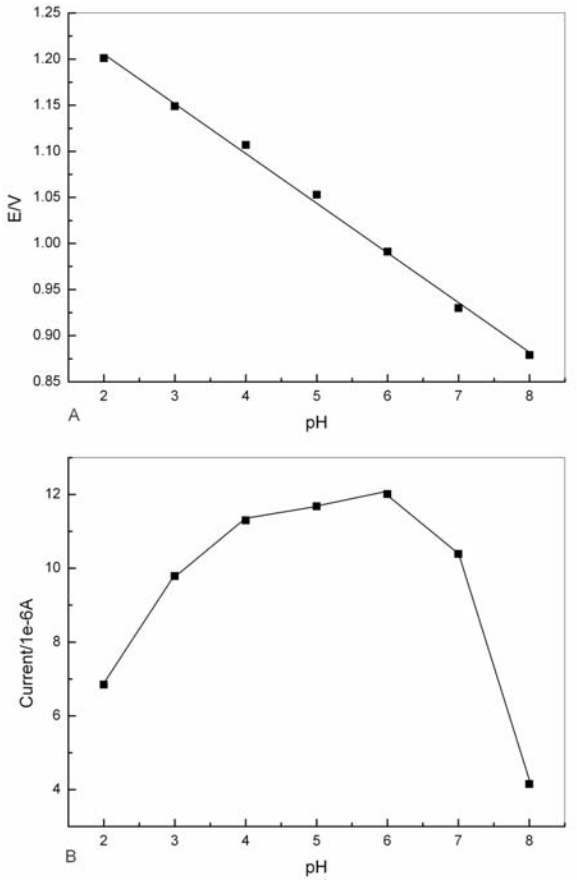

Figure 4. A: Relationship between the peak potential and pH; B: Relationship between the peak current and pH.

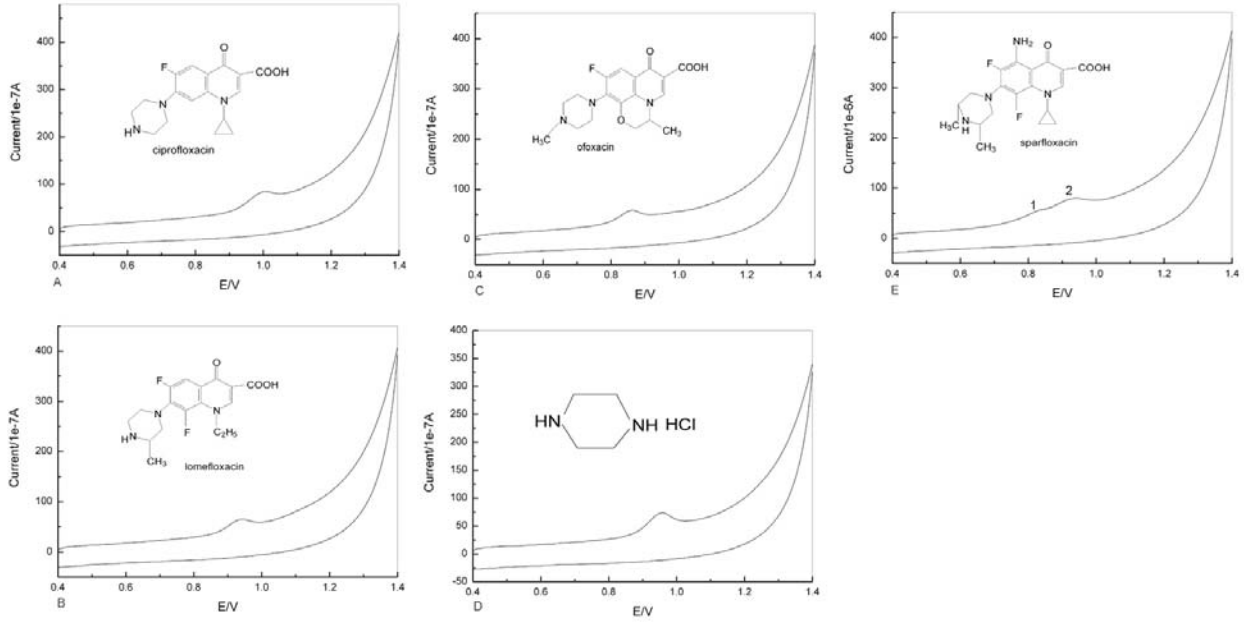

Figure 5. Cyclic voltammograms of 2×10^{-5} M different fluoroquinolone antibacterial agents and piperazine hydrochloric acid at a bare GCE in 0.1M PBS (pH 6.0).

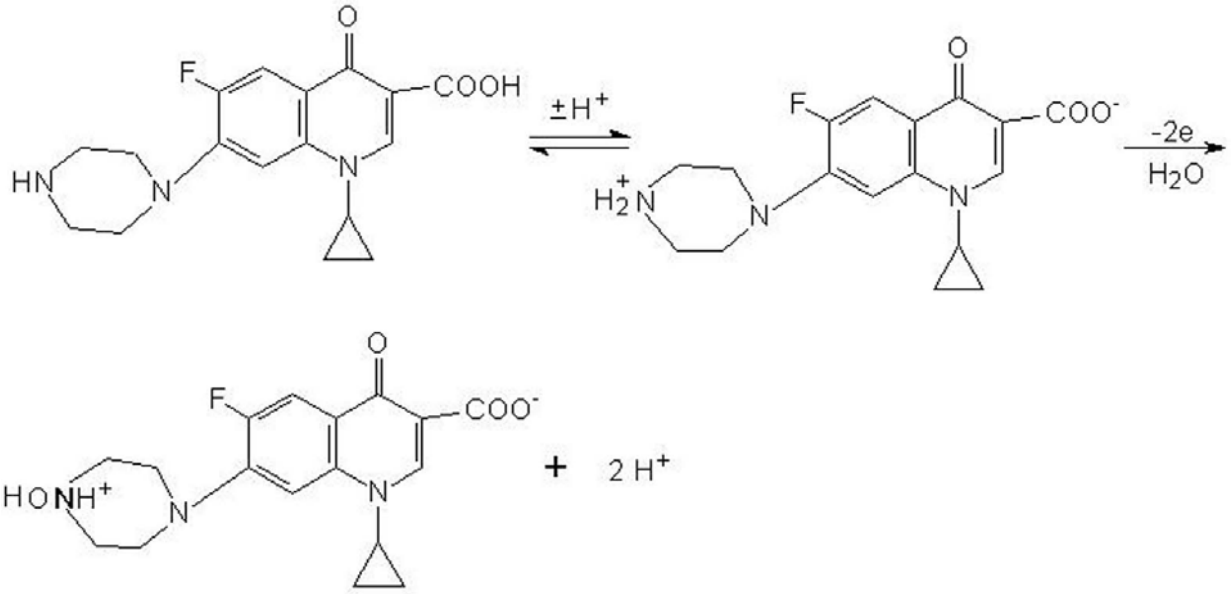

Figure 6. The eletrooxidation mechanism of CFX.

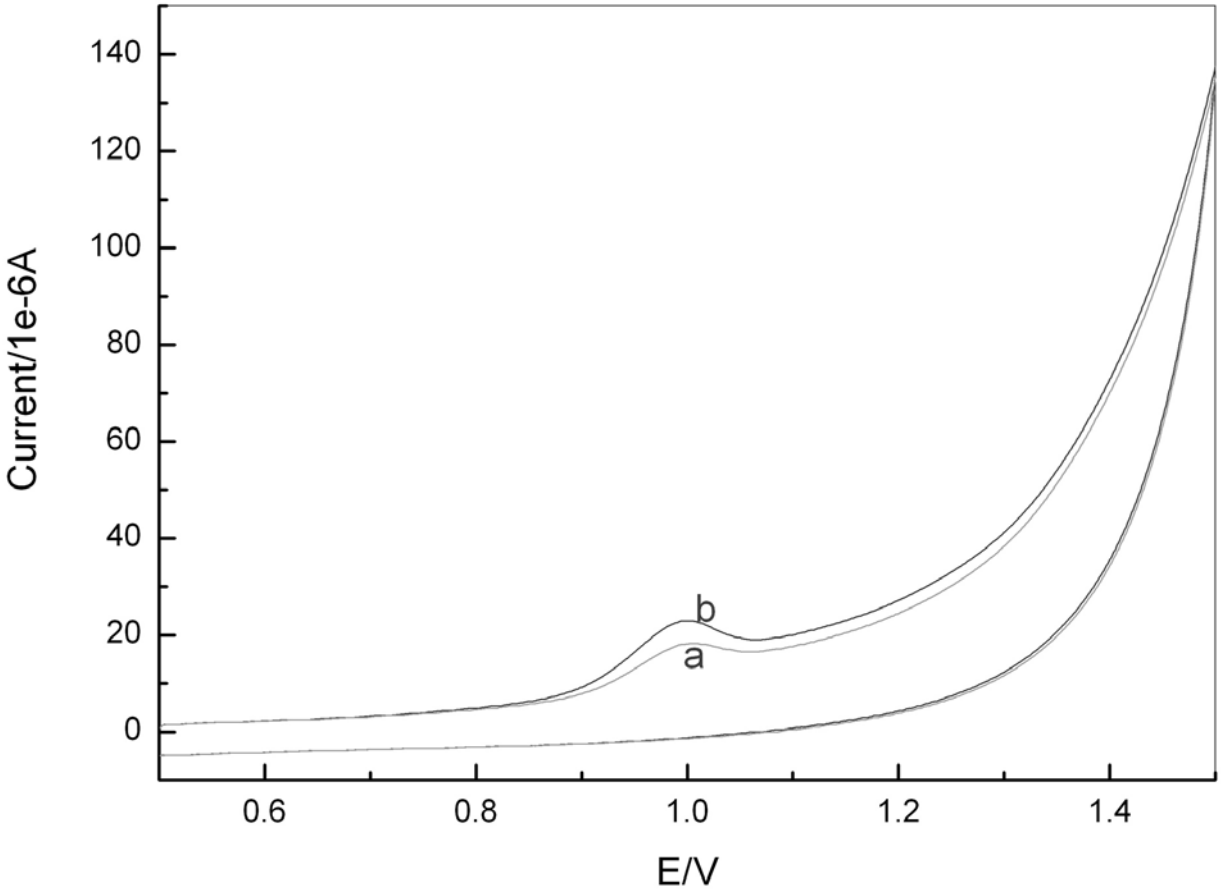

Figure 7. Cyclic voltammograms of 0.1M PBS (pH6.0) containing 1×10^{-5} M CFX in the absence of (b) and presence of 2×10^{-5} M DNA (a) .

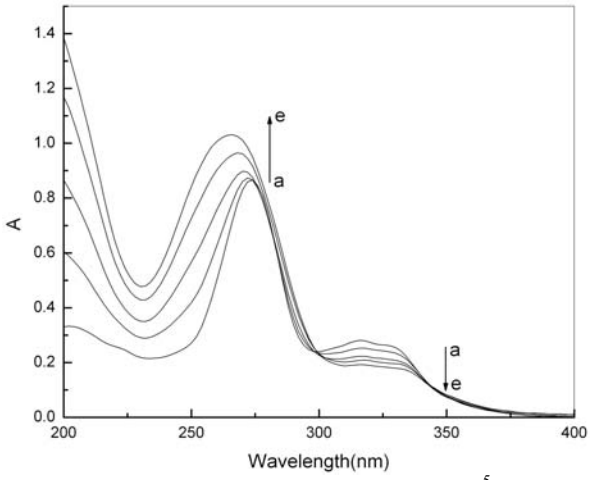

Figure 8. UV/Vis absorption spectra of 1.5×10^{-5} M CFX and different concentrations of DNA (a) 0 M (b) 1.0×10^{-5} M (c) 2.0×10^{-5} M (d) 3.0×10^{-5} M (e) 4.0×10^{-5} M .

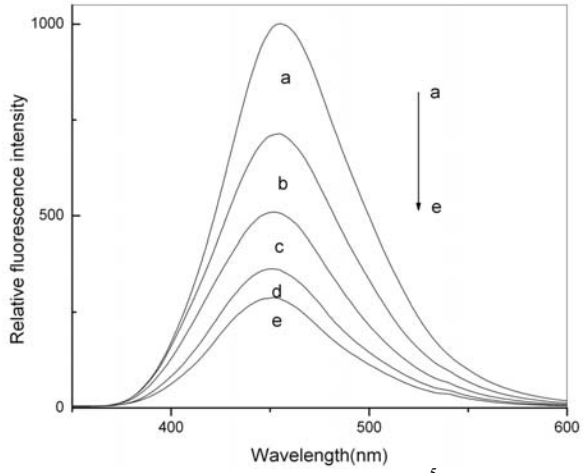

Figure 9. Fluorescence emission of 1.5×10^{-5} M CFX and different concentrations of DNA (a) 0 M (b) 1.0×10^{-5} M (c) 2.0×10^{-5} M (d) 3.0×10^{-5} M (e) 4.0×10^{-5} M.

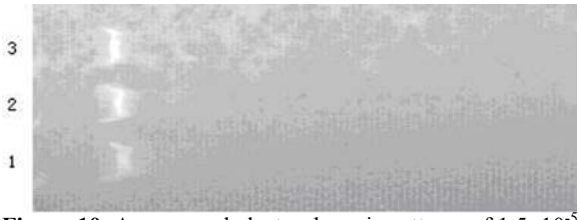

Figure 10. Agarose gel electrophoresis patterns of 1.5×10^{-5} M DNA and various concentration of CFX. (1) 2×10^{-6} M, (2) 2×10^{-5}M, (3) 2×10^{-4} M.

decreased (Curve b-e). Accompanying the binding process one-isosbestic point appeared which indicated the conformation of the ctDNA-CFX was homogeneous. It has suggested that hypochromism is a consequence of interactions between the electronic states of the intercalating chromophore and that of the ctDNA base pairs (34). These spectral changes, e.g. hypochromicity, red shift, and isobestic point, are consistent with the chromophore intercalating into the ctDNA base pairs. From the observations detailed above, we surmised that the intercalation occurred.

4.3.3. Studying fluorescence spectra

The interaction of CFX and ctDNA was also examined by fluorescence spectra. The fluorescent emission spectra of CFX and the effect of ctDNA concentrations on the fluorescence emission spectra of CFX are illustrated in Figure 9. CFX exhibited an emission maximum at 449 nm (Fig.9. a). The fluorescence emission was gradually decreased with increasing amount of ctDNA (curve b-e), showing that the CFX fluorescence was efficiently quenched upon binding to ctDNA. The stronger quenching of ciprofloxacin fluorescence without significant shift could originate in guanine (the oxidation potential of guanine is the lowest in nucleobases). Also, guanine could be an effective quencher of fluorescence through electron transfer from DNA to photo-excited fluoroquinolone □29□ . Norfloxacin have been well recorded □33, 35-37□. When norfloxacin bound to DNA or synthetic polynucleotide, the intensity of fluorescence decreased without changing the shape upon binding to DNA or poly $(d(G-C)_2)$, however, emission maximum red shifted with an isosbestic wavelength when it bound to poly $(d(I-C)_2)$ and poly $(d(A-T)_2)$. From these fluorescence results and other observations, Authors thought norfloxacin bound in the minor groove of native DNA and poly $(d(G-C)_2)$, which had the possibility of partial intercalation between amine group at the 2-position of guanine base and oxygen atoms of norfloxacin. The chromophore of norfloxacin and CFX is identical; hence similar spectral properties for both compounds are expected if they bind to native DNA with the similar binding mode. This is agreement with that clarified in absorption spectra and the electrochemical methods.

4.3.4. Agarose gel electrophoresis

Agarose gel electrophores is a generally separating, identifying, purifying DNA method. For more confirmation the mode of CFX and ctDNA action, an agarose gel electrophoresis had also been done. The patterns are shown in Figure 10. The ctDNA was dyed by the CFX and not ethidium bromide (EB) which was a typical intercalater. The Figure 10 was the patterns of 1.5×10^{-5} M ctDNA and different CFX (2×10^{-6}M, 2×10^{-5} M, 2×10^{-4} M from 1 to 3). The electrophoresis speeds became slower and the patterns were more luminous with the CFX concentration increasing. The reason could be due to much more ctDNA-CFX adduct forming so that the molecular electrophoresis speeds were slower and the dyed ctDNA were more. The experiment indicates CFX is similar to EB and could intercalate into the bases of ctDNA. If the binding of CFX and ctDNA only was an electrostatic interaction or groove binding, positive charge CFX should shift to the cathode of the electrophoresis trough, so ctDNA was not dyed. The result forcefully supported the intercalating mode of CFX and ctDNA.

4.3.5. Quenching studies

Another fact that supported the intercalation mechanism comes from determining the relative

fluorescence intensity of the free and bound CFX when potassium iodide existed. If CFX intercalated into the helix it should be protected, owing to the base pairs above and below. Whereas single groove binding or electrostatic interaction could expose the binding molecules much more than the intercalating species, it should provide much less protection (38). This was consistent with our expectation of intercalation, when the anionic quenchers - potassium iodide were added in the solution; relative fluorescence quenching was found to be much smaller in the presence of ctDNA than its absence. Simple linear behavior was apparent from the quenching curves, this indicated the interaction of CFX and ctDNA was only one major binding mode, which was the intercalation. This was another forceful proof of intercalation mechanism.

5. CONCLUSIONS

In this paper, the nano-SnO_2/PVS film was cast onto the surface of GCE and the electrochemical behavior of CFX at the modified electrode was investigated. In addition the electrochemistry, agarose gel electrophoresis and spectroscopic methods were applied to investigate the interaction of CFX and ctDNA, which was an intercalation mechanism.

6. ACKNOWLEDGEMENTS

This project was supported by the Key Nature Science Foundation of Anhui province Ministry of Education (No. 2006KJ040A) and the Education Department (No. 2006KJ006TD) of Anhui Province.

7. REFERENCES

1. Acciawi M., C. Canevial, M. Mari, M. Mattoni, R. Ruffo, R. Scotti, F. Morazzoni, D. Barreca, L. Armelao and E. Tondello: Nanocrystalline SnO_2-Based Thin Films Obtained by Sol-Gel Route: A Morphological and Structural Investigation. *Chem Mater* 15, 2646-2650 (2003)
2. Yu K.N., Y.H. Xiong, Y.L. Liu and C.S. Xiong: Microstructural change of nano-SnO_2 grain assemblages with the annealing temperature. *Phys Rev B* 55, 2666-2671 (1997)
3. Topoglidis E., Y. Astuti, F. Duriaux, M. Gratzal and J.R. Durrant: Direct Electrochemistry and Nitric Oxide Interaction of Heme Proteins Adsorbed on Nanocrystalline Tin Oxide Electrodes. *Langmuir* 19, 6894-6900 (2003)
4. Topoglidis E., A.E.G. Cass, G. Gilard, S. Sadeghi, N. Beaumont and J.R. Durrant: Protein adsorption on Nanocrystalline TiO_2 Films: An Immobilization Strategy for Bioanalytical Devices. *Anal Chem* 70, 5111-5113 (1998)
5. Nadzhafova O.Y., V.N. Zaitser, M.V. Drozdiva, A. Vaze and J.F. Rusling: Heme proteins sequestered in silica sol–gels using surfactants feature direct electron transfer and peroxidase activity. *Electrochem Commun* 6, 205-209 (2004)
6. Wang Q.L., G.X. Lu and B.J. Yang: Myoglobin/Sol-Gel Film Modified Electrode: Direct Electrochemistry and Electrochemical Catalysis. *Langmuir* 20, 1342-1347 (2004)
7. Kasmi A.E., M.C. Leopold, R. Galligan, R.T. Robertson, S.S. Saavedra, K.E. Kacemi and E.F. Bowden: Adsorptive immobilization of cytochrome *c* on indium/tin oxide (ITO): electrochemical evidence for electron transfer-induced conformational changes. *Electrochem Commun* 4, 177-181 (2002)
8. Willit J.L. and E.F. Bowden: Adsorption and redox thermodynamics of strongly adsorbed cytochrome c on tin oxide electrodes. *J Phys Chem* 94, 8241-8246 (1990)
9. Leger C., S.J. Elliott, K.R. Hoke, L.J.C. Jenken, A.K. Jones and F.A. Armstrong: Enzyme Electrokinetics: Using Protein Film Voltammetry To Investigate Redox Enzymes and Their Mechanisms. *Biochemsitry* 42, 8653-8662 (2003)
10. Mckenzie K.J. and F. Marken: Accumulation and Reactivity of the Redox Protein Cytochrome *c* in Mesoporous Films of TiO_2 Phytate. *Langmuir* 19, 4327-4331 (2003)
11. He P.L., N. Hu and J.F. Rusling: Driving Forces for Layer-by-Layer Self-Assembly of Films of SiO_2 Nanoparticles and Heme Proteins**.** *Langmuir* 20, 722-729 (2004)
12. Armstrong F.A. and G.S. Wilson: Recent developments in faradaic bioelectrochemistry. *Electrochim Acta* 45, 2623-2645 (2000)
13. Dai Z.H., S.Q. Liu, H.X. Ju and H.Y. Chen: Direct electron transfer and enzymatic activity of hemoglobin in a hexagonal mesoporous silica matrix. *Biosens Bioelectron* 19, 861-867 (2004)
14. Li Q.W., G.A. Luo and J. Feng: Direct Electron Transfer for Heme Proteins Assembled on Nanocrystalline TiO_2 Film. *Electroanalysis* 13, 359-363 (2001)
15. Drlica K: Mechanism of fluoroquinolone action. *Curr Opin Microbiol* 2, 504–508 (1999)
16. Fan J.Y., D. Sun, H. Yu, S.M. Kerwin and L.H. Hurley: Self-assembly of a quinobenzoxazine–Mg^{2+} complex on DNA: a new paradigm for structure of a drug–DNA complex and implications for the structure of the quinolone bacterial gyrase–DNA complex. *J Med Chem* 38, 408– 424 (1995)
17. Palù G, S. Valisena, G. Ciarrocchi, B. Gatto and M. Palumbo: Quinolone binding to DNA is mediated by magnesium ions. *Proc Natl Acad Sci U S A* 89, 9671–9675 (1992)
18. Sissi C, M. Andreolli, V. Cecchetti, A. Fravolini, B. Gatto and M. Palumbo: Mg^{2+}-mediated binding of 6-substituted quinolones to DNA: relevance to biological activity. *Bioorg Med Chem* 6, 1555–1561 (1998)
19. Sissi C, E. Perdona, E. Domenici, A. Feriani, A.J. Howells, A. Maxwell and M. Palumbo: Ciprofloxacin affects conformational equilibria of DNA gyrase in the presence of magnesium ions. *J Mol Biol* 311,195– 203 (2001)
20. Shen L.L., J. Baranowski and A.G. Pernet: Mechanism of inhibition of DNA gyrase by quinolone antibacterials: specificity and cooperativity of drug binding to DNA. *Biochemistry* 28, 3879– 3885 (1989)
21. Shen L.L., L.A. Mitscher, P.N. Sharma, T.J. O'Donnell, D.W.T. Chu, C.S. Cooper, T. Rosen and A.G. Pernet: Mechanism of inhibition of DNA Gyrase by quinolone antibacterials: a cooperative drug–DNA binding model. *Biochemistry* 28, 3886– 3894 (1989)

22. Palumbo M, B. Gatto, G. Zagatto and G. Palù: On the mechanism of action of quinolone drugs. *Trends Microbiol* 1, 232– 235 (1993)
23. Critchlow S.E. and A. Maxwell: DNA cleavage is not required for the binding of quinolone drugs to the DNA gyrase–DNA complex. *Biochemistry* 35, 7387– 7393 (1996)
24. Barton J.K., J.M. Goldberg, C.V. Kumar and N.J. Turro: Binding modes and base specificity of tris (phenanthroline) ruthenium (II) enantiomers with nucleic acids: tuning the stereoselectivity. *J Am Chem Soc* 108, 2081-2088 (1986)
25. Jia N.Q., Q. Zhou, L. Liu, M.M Yan and Z.Y. Jiang: Direct electrochemistry and electrocatalysis of horseradish peroxidase immobilized in sol–gel-derived tin oxide/gelatin composite films. *J Electroanal Chem* 580, 213-221(2005)
26. Lee D.S., H.J. Han, K. Kim, W.B. Park, J.K. Cho and J.H. Kim: Dissociation and complexation of fluoroquinolone analogues. *J Pharm Biomed Anal* 12, 157–164 (1994)
27. Turel I., N. Bukovec and E. Farkas: Complex formation between some metals and a quinolone family member (ciprofloxacin). *Polyhedron* 15, 269–275 (1996)
28. Turel I., P. Bukovec and M. Quiròs: Crystal structure of ciprofloxacin hexahydrate and its characterization. *Int J Pharm* 152, 59– 65 (1997)
29. Larsson A., C. Carlsson and M. Jonsson: Characterization of the binding of YO to [poly (dA– dT)]$_2$ and [poly(dG– dC)]$_2$, and of the fluorescent properties of YO and YOYO complexed with the polynucleotides and double stranded DNA. *Biopolymers* 36, 153–167 (1995)
30. Smyth W.F. and A. Ivaska: A study of the electrochemical oxidation of some 1, 4-benzodiazepines. *Analyst* 110, 1377-1379 (1985)
31. Kauffmann J.M, J.C. Viré, G.J. Patriarche, L.J. Nunez-Vergara and J.A. Squella: Voltammetric oxidation of trazodone. *Electrochim Acta* 32, 1159-1162 (1987)

32. Uslu B.and S.A.Ö. zkan: Electrochemical characterisation of nefazodone hydrochloride and voltammetric determination of the drug in pharmaceuticals and human serum. *Anal Chim Acta* 462, 49-57 (2002)

33. Gwan S. S, J.A. Yeo, M.S. Kim, S.K. Kim, A. Holmén, B. Åkerman and B. Nordén: Binding Mode of Norfloxacin to Calf Thymus DNA. *J Am Chem Soc* 120, 6451-6457 (1998)

34. Long E.C. and J.K. Barton: On demonstrating DNA intercalation. *Acc Chem Res* 23, 271-273 (1990)
35. Gwan S. S, J.A. Yeo, J.M. Kim, S.K. Kim, H.R. Moon and W. Nam: Base specific complex formation of norfloxacin with DNA. *Biophys Chem* 74, 225-236 (1998)
36. Lee E.J., J.A. Yeo, C.B. Cho, G.J. Lee, S.W. Han and S.K. Kim: Amine group of guanine enhances the binding of norfloxacin antibiotics to DNA. *Eur J Biochem* 267, 6018-6024 (2000)
37. Lee E.J., J.A. Yeo, K. Jung, H.J. Hwangbo, G.J. Lee and S.K. Kim: Enantioselective Binding of Ofloxacin to B Form DNA. *Arch Biochem Biophys* 395, 21-24 (2001)
38. Kumar C.V., R.S. Turner and E.H. Asuncion: Groove binding of a styrylcyanine dye to the DNA double helix: the salt effect. *J Photochem Photobiol A: Chem* 74, 231-238 (1993)

Abbreviations: GCE: glassy carbon electrode, PVS: poly vinyl sulfonic potassium, PBS: phosphate buffer solutions, CFX: ciprofloxacin, TEM: transmission electron microscopy, XRD: X-ray diffraction, CVs: cyclic voltammograms, DPV: differential pulse voltammetry, OFX: ofloxacin, SPX: sparfloxacin, LMX: lomefloxacin

Key Words: Ciprofloxacin, ctDNA, nano-SnO_2, Poly (Vinyl) Sulfonic Potassium, Interaction

Send correspondence to: Dr Yuzhong Zhang, College of Chemistry and Materials Science, Anhui Normal University, Wuhu 241000, P.R. China, Tel: 86-553-3869303, Fax: 86-553-3869303, E-mail: zhangyz65@hotmail.com

http://www.bioscience.org/current/vol12.htm